Spin polarization of graphene on $Co_2FeGe_{0.5}Ga_{0.5}$(001) observed by spin-polarized surface positronium spectroscopy

A. Miyashita, S. Li, S. Sakai, M. Maekawa, and A. Kawasuso*

National Institutes for Quantum and Radiological Science and Technology, 1233 Watanuki, Takasaki, Gunma 370-1292, Japan

(Received 3 May 2020; revised 12 July 2020; accepted 13 July 2020; published 27 July 2020)

Following previous work on graphene on Ni(111) and Co(0001) surfaces [Phys. Rev. B **97**, 195405 (2018)], the spin polarization of graphene on a $Co_2FeGe_{0.5}Ga_{0.5}$ (CFGG) (001) surface was examined using spin-polarized surface positronium spectroscopy. The graphene was found to be magnetically insulated from the CFGG(001) even after heat treatment, which increased the spin polarizations of graphene on Ni(111) and Co(0001). First-principles calculations indicated that graphene is weakly bound to the CFGG(001) surface mainly through the van der Waals interaction, and consequently the interlayer distance between graphene and the CFGG(001) surface is greater (∼3 Å) than that between graphene and Ni(111) or Co(0001) (∼2 Å). The weak hybridization between graphene and CFGG(001) sufficiently reduces the spin polarization in graphene, which enables the magnetic insulation of graphene from CFGG.

DOI: 10.1103/PhysRevB.102.045425

I. INTRODUCTION

The extremely high carrier mobility and long spin diffusion length in graphene mean that graphene and ferromagnet heterostructures are receiving extensive research interest in the contexts of spintronic device applications and solid-state physics [1].

Spin-polarized carriers are induced into graphene in two ways. One is to magnetize the graphene itself through the magnetic proximity effect. Previous work has shown that graphene on Co(0001) and Ni(111) can be magnetized sufficiently because of the strong hybridization at the interfaces [2,3]. The other way is to inject excess spins from a ferromagnet into graphene under an electric bias [4–6]. In such a vertical spin valve configuration, the graphene middle layer should be magnetically insulated from the ferromagnet; that is, the hybridization between the graphene and the ferromagnet must be suppressed. As a candidate ferromagnet, the half-metallic Heusler alloy $Co_2FeGe_{0.5}Ga_{0.5}$ (CFGG) has been proposed recently [7].

Confirming the magnetic insulation of graphene from CFGG requires the surface spin polarization of graphene-CFGG to be measured, which to the best of our knowledge has not been done until now. In this work, we used spin-polarized surface positronium spectroscopy because it is guaranteed to detect the electron spin polarization of the first surface layer [8–11]. The results show that the surface spin polarization of graphene-CFGG(001) is below the detection limit, and also that a relatively large interlayer spacing forms at the interface. First-principles calculations confirm that these results originate from the weak hybridization between graphene and the CFGG(001) surface.

II. EXPERIMENT

A 20-nm-thick CFGG(001) thin film was grown on MgO(001) by magnetron sputtering, after which graphene was grown on it by ultra-high-vacuum chemical vapor deposition [7]. The sample was transferred in air to a vacuum chamber with a base pressure below 10^{-7} Pa and equipped with a positron beam apparatus. X-ray magnetic circular dichroism measurements confirmed that the degradation of the CFGG surface during the transportation in air was negligibly small [7]. The CFGG layer was magnetized in-plane along its easy axis [110] in a magnetic field of 30 mT, and all the measurements were conducted in the magnetic remanent state. Transversely spin-polarized positrons with an energy of 200 eV were injected into the sample. Some of the positrons diffused back to the surface and were emitted into the vacuum as positronium having picked up surface electrons. From the three-photon annihilation events of positronium and the two-photon annihilation events of positronium and free positrons measured with a high-purity Ge detector, the positronium fraction I_{Ps} (number ratio of emitted positronium to implanted positrons) [12–14] was obtained for positive and negative magnetization directions ($\pm M$) with respect to the positron spin polarization. The surface spin polarization was determined as

$$P_- = \frac{1}{\alpha P_+}\frac{I_{Ps}(-M) - I_{Ps}(+M)}{I_{Ps}(-M) + I_{Ps}(+M)} = \Delta P_-(-M) - \Delta P_-(+M),$$

where P_+ (=0.3) is the positron spin polarization, α (=0.6) is the coefficient determined from the spin-dependent detection efficiency of annihilation photons [15], and $\Delta P_-(\pm M)$ is the shift of $I_{Ps}(\pm M)$ from its middle point divided by $\alpha P_+[I_{Ps}(-M) + I_{Ps}(+M)]$, that is, the shift of the spin polarization from the nonmagnetized state. In each experiment, eight spectra were recorded, four for the positive direction

*Corresponding author: kawasuso.atsuo@qst.go.jp

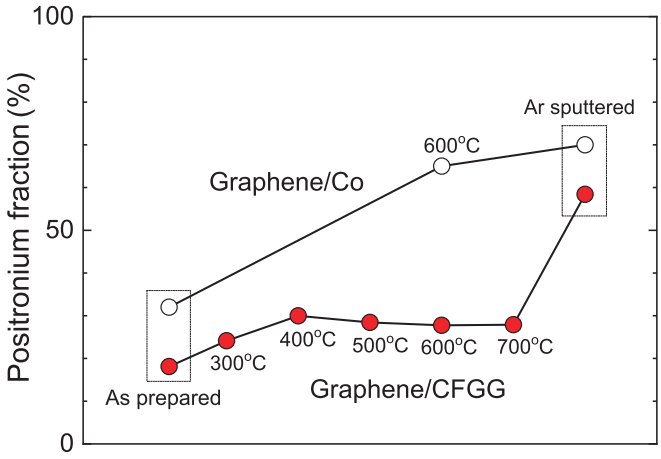

FIG. 1. Positronium fractions obtained for graphene-CFGG(001) and graphene-Co(0001) surfaces in their as-prepared states and after annealing up to 700 °C and 1 keV Ar ion sputtering.

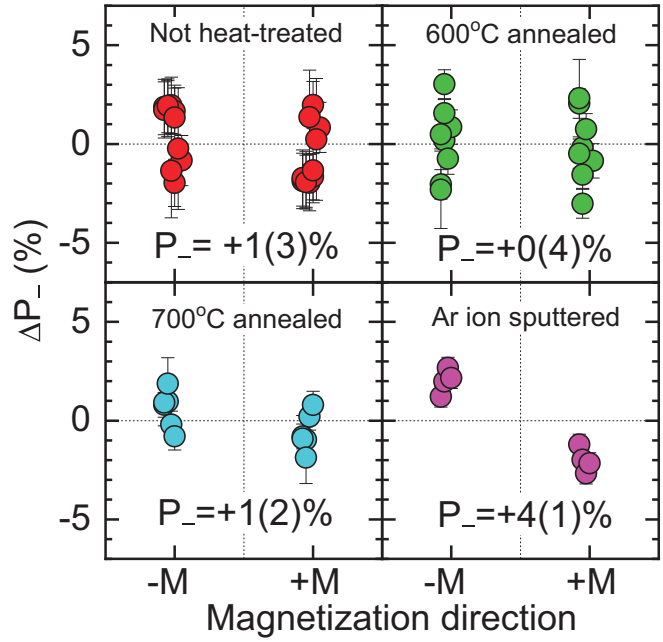

FIG. 2. Spin polarizations obtained for graphene-CFGG(001) surface in its as-prepared state and after annealing up to 700 °C and 1 keV Ar ion sputtering. The vertical axis is the shift of the spin polarization for positive ($+M$) and negative ($-M$) magnetizations (see text). The net spin polarization $[\Delta P_{-}(-M) - \Delta P_{-}(+M)]$ is indicated in each panel. The numbers in parentheses indicate errors.

and four for the negative direction. This protocol was repeated between five and eight times. In each spectrum, a total count of 4×10^5 was accumulated. The details are described elsewhere [3].

III. THEORETICAL CALCULATION

To interpret the experimental data quantitatively, density-functional theory calculations were carried out using the ABINIT code [16] with the projector-augmented-wave method [17] within the generalized gradient approximation [18]. The initial valence electron configurations were assumed to be $3s^2 3p^6 3d^8 4s^1$ (Co), $3s^2 3p^6 3d^7 4s^1$ (Fe), $3d^{10} 4s^2 4p^1$ (Ga), $3d^{10} 4s^2 4p^2$ (Ge), and $2s^2 2p^2$ (C). The positronium work function of CFGG was calculated as $\Phi_{\mathrm{Ps}} = -A_+ - 6.8$ eV, where A_+ is the positron affinity, with the primitive cell and the k-point sampling of $5 \times 5 \times 3$ under full structural optimization. For the surface state calculation, a CFGG(001) film was constructed with seven monolayers and a 3×1 cell in the surface parallel direction. The top layer was composed of Fe, Ga, and Ge atoms, while the second layer was composed of only Co atoms. The graphene layer with a 8×2 cell was placed on the CFGG surface. The back surfaces were treated in the same way to avoid any artificial effects arising from asymmetry. The van der Waals potential was also considered [19]. The initial vacuum layer was 20 Å. For the electron calculation, the k-point sampling number was $2 \times 5 \times 1$. For the positron calculation, only the Γ point was considered. Full structural optimization was also carried out.

IV. RESULTS AND DISCUSSION

A. Experiment

Figure 1 shows the positronium fractions obtained for graphene-CFGG(001) in its as-prepared state and after annealing up to 700 °C and Ar ion sputtering for 10 s to remove the graphene layer. As a reference, the data obtained for graphene-Co(0001) are also plotted [3]. For the graphene-Co, the positronium fraction increases from ∼30% in the as-prepared state to more than ∼65% upon annealing at 600 °C and to ∼70% after Ar ion sputtering. The first increase by annealing means that some of the adsorbates put on the graphene during the transportation in air are desorbed, resulting in sufficient positronium emission. The second increase after removing the graphene indicates that the positronium emission is not restricted so much by the graphene layer. By contrast, for the graphene-CFGG, the positronium fraction in the as-prepared state is less than 20%, increases by at most 10% by the annealing up to 700 °C, and increases to ∼60% after the Ar ion sputtering. This means that the graphene layer prevents the positronium emission for reasons that are discussed later.

Nevertheless, because the positronium fraction is not zero, the spin polarization can be measured. Figure 2 shows the plots of $\Delta P_{-}(\pm M)$ in the as-prepared state, after annealing, and after removing the graphene layer by Ar ion sputtering. For the as-prepared and annealed states, the obtained spin polarizations are either zero or very small and positive ($< 1\%$), although the data error and scattering are rather large because of the low positronium fraction. This result is in contrast to the results for graphene-Co(0001) and graphene-Ni(111). For the Ar-ion-sputtered state, the data error and scattering are suppressed, and $P_{-} = +4\%$ is obtained as the spin polarization of the CFGG surface.

The above results are summarized as follows: (1) the positronium emission from graphene-CFGG is inefficient and (2) the spin polarization induced in graphene-CFGG is much lower than that in graphene-Co(0001) and graphene-Ni(111). These two results are interpreted by the theoretical calculations in Sec. IV B.

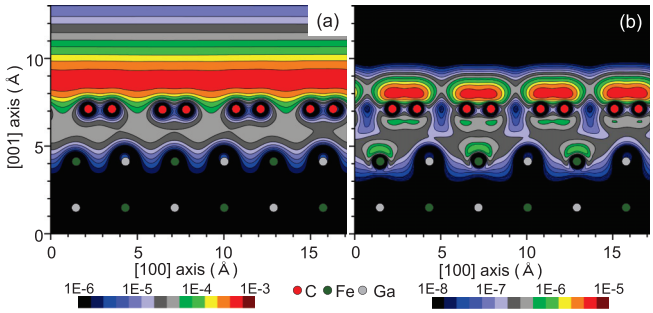

FIG. 3. Cross-sectional distributions of (a) positron density in a_B^{-3} and (b) electron-positron density in a_B^{-6} calculated for graphene-CFGG(001) on the (010) plane. The red, green, and gray circles denote C, Fe, and Ga atoms, respectively.

B. Theoretical interpretation

The interlayer distance between the graphene and CFGG(001) top layer was determined to be 2.9 Å. The average buckling of C atoms was 0.1 Å. Compared to graphene-Co(0001) and graphene-Ni(111), [3] the interlayer distance is approximately 1 Å greater, while the buckling is nearly the same. These confirm the previous prediction that graphene is weakly bound to the CFGG(001) surface mainly through the van der Waals interaction and its flat structure is maintained [7].

The positronium work function for CFGG was calculated to be −4.9 eV, suggesting that positronium is emitted spontaneously from the CFGG surface. This explains the higher positronium fraction observed for the CFGG(001) surface after removing the graphene. Because the positronium work function is basically unaltered by surface adsorbates, positronium may be emitted efficiently from graphene-CFGG. However, the experiment shows only a limited positronium fraction. As shown in Fig. 3(a), apart from the vacuum region where positrons prefer to stay, there is a finite positron density between the graphene and the CFGG(001) top layer. This is caused by the formation of a trapping potential because of the long interlayer distance between the graphene and the CFGG. Positrons propagating from deeper regions are probably trapped by the potential, thereby reducing their transmission to the vacuum. Consequently, the positronium formation may be suppressed. This explains the low positronium fraction observed for graphene-CFGG(001).

The relatively large interlayer distance between the graphene and the CFGG(001) top layer is caused by the weak hybridization among their electronic states. Indeed, as shown in Fig. 4(a), the present band calculations show that the Dirac cone dispersion of graphene remains conserved in the contact with the CFGG surface. Consequently, the magnetic proximity effect of CFGG on graphene is weak. This explains qualitatively the observed low-spin polarization of graphene on CFGG.

For a more quantitative explanation, we require the electron density of states (DOS) in the region where positronium forms efficiently. Figure 3(b) shows that the electron-positron overlap density is higher just outside the graphene layer. This suggest that the positronium formation probability is higher there. Therefore, we computed the electron-positron DOS (e-p DOS), which is defined as the local electron DOS weighted by the positron density [3]. Figure 4(b) shows the e-p DOS calculated for the graphene-CFGG(001) and CFGG(001) surfaces as a function of the electron energy E. The Dirac point of graphene shifted to $E \sim -1.2$ eV [Fig. 4(a)] is maintained in the e-p DOS. For CFGG(001), the sp bands were predominant down to $E \sim -1$ eV, and the d bands with more states took

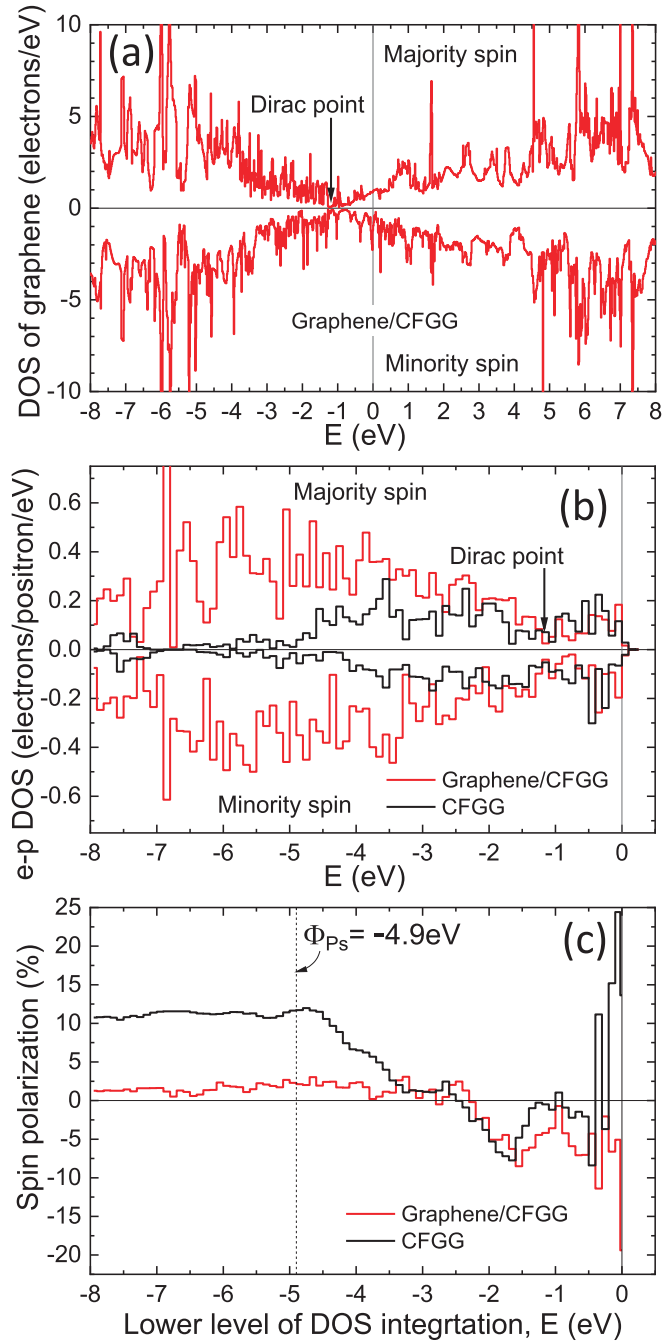

FIG. 4. (a) Electron density of states around graphene layer on CFGG(001). (b) Electron-positron density of states (e-p DOS) calculated for graphene-CFGG(001) (red) and CFGG(001) (black). (c) Electron spin polarizations calculated from the above e-p DOS as a function of the lower level of integration in e-p DOS. The Fermi level corresponds to $E = 0$. The broken line denotes the position of the calculated positronium work function of CFGG.

over down to $E \sim -5$ eV [7]. However, as seen in Fig. 4(b), the e-p DOS has a somewhat homogeneous distribution. This is because positrons have more (resp. less) overlapping with spatially delocalized (resp. localized) sp (resp. d) electrons, and thus the difference of state numbers for the sp and d bands is compensated for.

When positronium is formed via the work function mechanism, positrons can capture electrons in the energy range of $E = 0$ to $\Phi_{\rm Ps}$. The spin polarization detected by positronium spectroscopy should be compared with $P_- = \int_{\Phi_{\rm Ps}}^{0} \{D^{\uparrow}(E) - D^{\downarrow}(E)\}\, dE$, where $D(E)^{\uparrow(\downarrow)}$ is the e-p DOS of the majority (resp. minority) spin channel and $\int_{\Phi_{Ps}}^{0} \{D^{\uparrow}(E) + D^{\downarrow}(E)\}\, dE = 1$. Figure 4(c) shows the calculated electron spin polarization as a function of the lower level of integration. Although the spin polarization for CFGG(001) is $\sim$12% at $E = \Phi_{\rm Ps}$, it is reduced to $\sim$2% for graphene/CFGG(001). This explains the observed very low spin polarization for graphene-CFGG(001). Figure 4(c) shows the spin polarization of $\sim -5\%$ near the Fermi level. However, it may be practically difficult to expect a finite spin polarization near the Fermi level because the observed spin polarization is very low. For stricter evaluation of the Fermi-level spin polarization, we are currently developing an energy-resolved Ps spectroscopy. The observed spin polarization for the CFGG(001) surface, namely, $P_- = +4\%$, is lower than the calculated value. Possible reasons for this are (1) the degradation of CFGG regularity upon Ar sputtering and (2) the difficulty in keeping the surface clean during the measurements [20].

V. SUMMARY

Spin-polarized surface positronium spectroscopy has shown the spin polarization of graphene on CFGG(001) to be very low. This is explained by the weak interlayer exchange coupling between graphene and CFGG due to the weak van der Waals interaction. Because of this, the original Dirac cone of graphene may be well maintained. The preservation of the half-metallic nature of CFGG and the quasi-free-standing characteristics of graphene offers two prospects. One is the injection of spins from CFGG into graphene under an electric bias, taking advantage of the possibility that the spin polarization of conduction electrons in graphene is unaltered by strongly hybridized interface states. Another is the fabrication of graphene-CFGG-based vertical spin valve devices, given that the middle graphene layer is magnetically insulated from the CFGG layer.

ACKNOWLEDGMENT

This work was financially supported by JSPS KAKENHI under Grants No. 17K19061 and 20K05454.

[1] N. Tombros, C. Jozsa, M. Popinciuc, H. T. Jonkman, and B. J. van Wees, Nature (London) **448**, 571 (2007).
[2] S. Entani, M. Kurahashi, X. Sun, and Y. Yamauchi, Carbon **61**, 134 (2013).
[3] A. Miyashita, M. Maekawa, K. Wada, A. Kawasuso, T. Watanabe, S. Entani, and S. Sakai, Phys. Rev. B **97**, 195405 (2018).
[4] V. M. Karpan, G. Giovannetti, P. A. Khomyakov, M. Talanana, A. A. Starikov, M. Zwierzycki, J. van den Brink, G. Brocks, and P. J. Kelly, Phys. Rev. Lett. **99**, 176602 (2007).
[5] W. Li, L. Xue, H. D. Abruña, and D. C. Ralph, Phys. Rev. B **89**, 184418 (2014).
[6] M. Piquemal-Banci, R. Galceran, M. B. Martin, F. Godel, A. Anane, F. Petroff, B. Dlubak, and P. Seneor, J. Phys. D: Appl. Phys. **50**, 203002 (2017).
[7] S. Li, K. V. Larionov, Z. I. Popov, T. Watanabe, K. Amemiya, S. Entani, P. V. Avramov, Y. Sakuraba, H. Naramoto, P. B. Sorokin, and S. Sakai, Adv. Mater. **32**, 1905734 (2020).
[8] D. W. Gidley, A. R. Köymen, and T. W. Capehart, Phys. Rev. Lett. **49**, 1779 (1982).
[9] A. Kawasuso, Y. Fukaya, M. Maekawa, H. Zhang, T. Seki, T. Yoshino, E. Saitoh, and K. Takanashi, J. Mag. Mag. Mater. **342**, 139 (2013).
[10] H. J. Zhang, Y. Fukaya, M. Maekawa, H. Li, A. Kawasuso, T. Seki,, E. Saitoh, and K. Takanashi, Sci. Rep. **4**, 4844 (2014).
[11] H. J. Zhang, S. Yamamoto, B. Gu, H. Li, M. Maekawa, Y. Fukaya, and A. Kawasuso, Phys. Rev. Lett. **114**, 166602 (2015).
[12] S. Marder, V. W. Hughes, C. S. Wu, and W. Bennett, Phys. Rev. **103**, 1258 (1956).
[13] K. G. Lynn and D. O. Welch, Phys. Rev. B **22**, 99 (1980).
[14] P. G. Coleman, Sol. Stat. Phen. **28-29**, 179 (1992).
[15] R. M. Drisko, Phys. Rev. **102**, 1542 (1956).
[16] X. Gonze, J.-M. Beuken, R. Caracas, F. Detraux, M. Fuchs, G.-M. Rignanese, L. Sindic, M. Verstraete, G. Zerah, F. Jollet *et al.*, Comput. Mater. Sci. **25**, 478 (2002).
[17] P. E. Blöchl, Phys. Rev. B **50**, 17953 (1994).
[18] J. P. Perdew, K. Burke, and M. Ernzerhof, Phys. Rev. Lett. **77**, 3865 (1996).
[19] S. Grimme, J. Comput. Chem. **27**, 1787 (2006).
[20] H. Li, M. Maekawa, A. Miyashita, and A. Kawasuso, Defect Diffusion Forum **373**, 65 (2017).